Swansea University
Prifysgol Abertawe

College of Engineering

Coursework Submission Sheet

Coursework Title: Research Paper	**Student Number:** 866435
Coursework Number: n/a	**Name:** Kevin Elanjickal
Module Code: EG-353	**Email:** 866435@swansea.ac.uk
Module Title: Individual Research Project	**Degree Course:** Mechanical BEng
Submission Deadline: 4pm on 4th May 2018	
Your Supervisor: Dr Davide Deganello	

By submitting this coursework, I certify that this is all my own work.

Submission date 4/05/18

SPLD Students

Please indicate if you are officially recognised by the University as an SPLD student: YES/NO

Development of Printable RFID Device

Author: Kevin Elanjickal
Co-Author: Davide Deganello
Welsh Centre for Printing and Coating
College of Engineering
Swansea University
Swansea UK

***Abstract*—This paper investigates the potential use of flexography printing to produce a responsive passive UHF RFID tag. This paper will also investigate into the performance of the antenna and the substrate with the help of measuring its resistance and using surface topology. The ink used for flexography printing was a soluble nanoparticle silver ink. The design of the antenna was taken into consideration. This report gives the evaluation of the physical characteristics of the successfully printed antennas. It has been seen that when an anilox roll with a higher cell volume count was used, the resistance of the antenna decreases. It was also seen that when an anilox roll with a lower cell volume count was used, the line width of the antenna decreases. The reading range of the responsive tags increased as the size of the dipole increased.**

Keywords—RFID, Flexography, Antenna, Liquid NanoParticle Silver ink, Resistance, Surface Topology.

I. INTRODUCTION

RFID technology can be seen frequently on a day-to-day basis, from "contactless" payments to accessing the garage door, it has the potential to tap into an even bigger market through its integration into various other applications. However, the production costs are considerably high due to the amount of material used for manufacturing the antenna itself. The manufacturing cost of the antenna could be reduced with the use of additive manufacturing.

This paper will look into the production and performance of a printed passive UHF RFID tag. The antenna will be printed with the process of flexography. Two different substrate materials will be used to print the antennas with the use of surface topology to evaluate the print quality. The flexography machine will use three different anilox rolls to evaluate how the performance of the antenna varies by measuring the resistance between each pole of the dipole. Three different antenna designs will be used to evaluate the read range, with the aid of an RFID reader. This research aims to develop a working RFID tag, produced with a printing process. It will evaluate the print quality against PET and PP substrates. It will look into the analysis of antenna performances with varying anilox rolls. This research will also look into comparing the read ranges of three different antenna designs.

By the end of this research, the main outcome is to produce responsive RFID tags. The read range will be expected to be lower as the shape size of the dipole becomes more compact. The resistance of the antenna will be lower as the volume count of the used anilox roll is higher. Another expected outcome of this research would be that the PET substrates would have a better print quality than PP.

II. LITERATURE REVIEW

A. RFID Systems

A radio frequency identification (RFID) system operates within the 20 kHz to 300GHz range [1], known as the radio range. This system consists of two main parts: a reading device, which will be made up of a transceiver and a scanning antenna, and the RFID tag itself (the transponder), which consists of a chip and an antenna. Figure 1 gives a visual representation of the system. Common RFID tags are usually made of a microchip, memory and an antenna. For the system to work the desired item is first attached with the tag and then to monitor the tags, a RFID reader will send out radio waves. This technology is very similar to the commonly used barcodes system; however, barcodes need to be in the view of the reader, whereas even if an object has been placed between the tag and the reader, it can still be read as long as it is within the range of the tag. An RFID reader can be used to read multiple tags. [2]

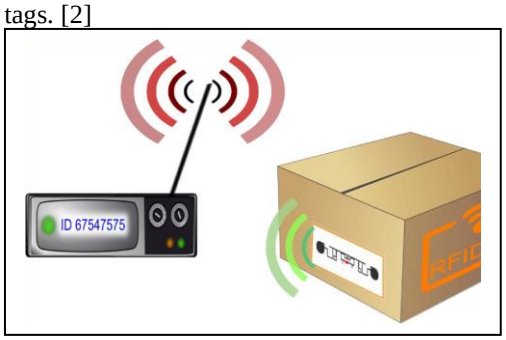

Figure 1. Visual Representation of RFID system. [3]

B. Types of RFID

There are three different types of tags; Active; Passive and Semi-Passive. The most commonly used tags, which are easily available in the market, are passive tags. Radio frequency (RF) waves power these tags, as it has no internal power. The passive tag then responds to the reader by sending out a modified RF wave to the reader. These tags have a reading range from 1 cm up to 15m. The memory stored within these tags is quite small when compared to active and semi-passive tags. Active tags have their own power source as well as the transmitter. Therefore, these tags can transmit its information to the reader without first receiving a signal from

the reader. These tags act as a beacon as it broadcasts its information constantly. Due to its internal power the reading range of these tags are boosted up to 200m and can also use a more powerful integrated circuit chip that gives a higher memory capacity when compared to passive tags. Semi-passive tags have an internal power, which powers up the integrated circuit chip but does not have the ability of transmitting RF waves on its own. The powered chip is concentrated on boosting the reading range up to 50m and help store more memory compared to passive tags. [4]

C. RFID Antennas

The variance of the RFID tag antennas depends on the application of the tag. The antenna design itself can also show some properties of the tag. Its design can show:

- The frequency of the tag
- The additional near field capabilities in case the tag is Far-field.
- The type of dipole antenna in case the tag uses an Ultra-High Frequency dipole

Due to the correlation between the design of the antenna and the used communication method, a visual examination of the antenna can determine the frequency range the tag operates within. The behaviour of the RF waves change depending on the operating frequency range. The three frequency ranges that work with RFID tags are; Low Frequency (LF); High Frequency (HF) and Ultra-High Frequency (UHF).

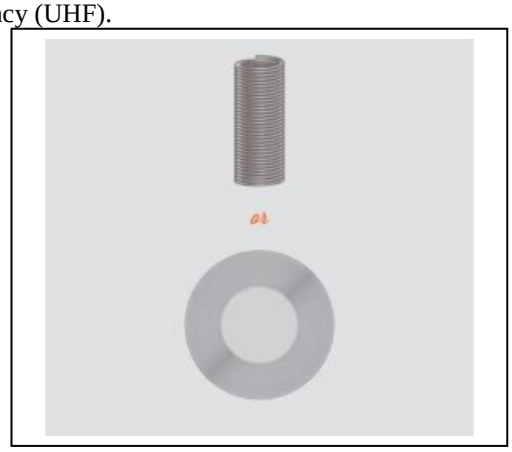

Figure 2. Low Frequency Antenna Design

LF types have a range between 125-135 kHz and have a read range from touch to 46cm. Inductive coupling is used for these tags, so the magnetic field, generated from the reader's antenna, activates an electric current in the tag's antenna. The design of the antenna is of a circular spiral coil tag shown in figure 2. Due to the long wavelength of LF waves, it has the ability to penetrate thin metallic materials. It can also read objects with high water content such as beverage cans. The applications for LF RFID tags include access control and animal tagging.

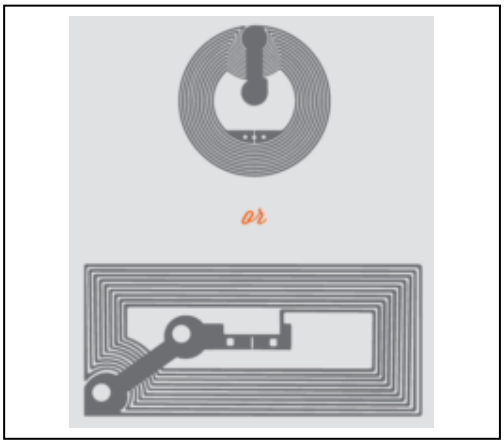

Figure 3. High Frequency Antenna Design

HF types have a frequency range from 13.553-13.567 MHz and have a read range from touch to around 1.5m. The use of inductive coupling allows the communication of HF tags with the reader. The antenna design of HF types are typically small in size, and in a rectangular or circular shape, as seen in figure 3. HF radio waves also have quite a good ability to penetrate metal and can work with items with medium to high water content. The applications of HF RFID tags include tracking library books, patient flow tracking and transit tickets.

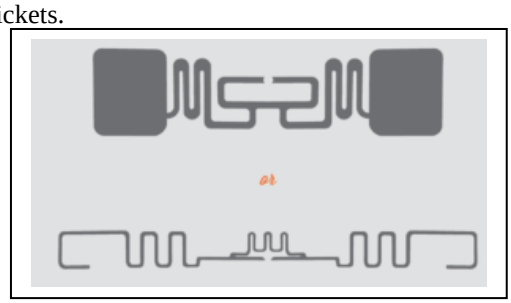

Figure 4. UHF Antenna Design.

UHF RFID tags have a frequency range from 400-1000 MHz and can read RF waves from touch to 50m. It uses backscatter coupling to communicate with the reader. The reader's antenna sends out RF waves and the RFID becomes active within the reading range. The tag then modulates the information and reflects the remaining energy back to the reader antenna. UHF tags use a dipole-shaped design for the antenna and if it contains a small loop in the centre, near field capabilities will be present. [5] Figure 4 shows a visual representation of the design. Due to its very high frequency, it will have a low wavelength so the signals sent out will be weaker than the other frequency ranges. Due to this, it cannot penetrate through metal and water but it will have a much quicker data transfer rate when comparing to HF and LF. Applications for UHF RFID tags are tracking inventory in warehouses as it passes through a door dock, tracking time as racers cross a reader on the finish line, electronic toll collection and parking access control. [6]

D. Manufacturing Methods of Printable RFID

Current prices for tracking specified RFID tags are still quite high. UHF RFID tags do not require thick antenna designs due to the occurrence of the skin effect. The skin effect is the behaviour of the alternating current of high frequencies, flowing only on the outer layer of the antenna and

closer to the surface of the tag. [7] Therefore, the thinner the antenna, the cheaper the cost of the tag. With new technology, RFID tags manufactured via additive layer manufacturing can show that it can be quite cost effective. There are various methods to make RFID tags with the aid of additive layer manufacturing. Additive manufacturing is the fabrication process of adding layer upon layer of material using 3D printing technology. [8]

Printing methodology is set into two classes: Non-Impact and Conventional. The non-impact printing process works around the basis of ink printing, which can be solvent, water based or UV cured. The four non-impact printing processes are ionography, thermography, electrophotography and inkjet. The use of ionography and thermography are not very popular when compared to the use of electrophotography and inkjet printing. The use of inkjet printing has been quite popular in research, however its major drawback is that it is temperature dependent. [9]

Conventional printing works with the use of a plate and an information-carrying medium. The three main conventional printing processes are screen-printing, gravure and flexography. [9] Electronic manufacturing commonly uses screen-printing. Screen printing works by pressing ink with a squeegee, forcing it to flow through a stencil and then printing it on to the substrate. Gravure printing works by pressing a substrate between a gravure cylinder, which will have the desired shape of the print, and an impression cylinder. [10]

E. Flexography

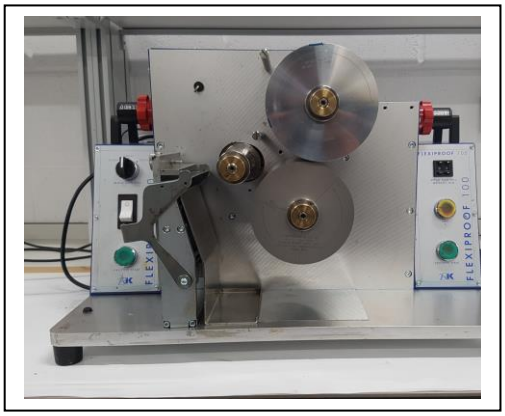

Figure 5. Laboratory Scale Flexography

Flexography is a rotary relief printing method using inks and plastic plates. In industry the substrate is fed through the system between the plate cylinder and the impression cylinder, however on a laboratory scale, the substrate is fastened to the impression cylinder. Figure 5 shows a laboratory scale flexography machine. The ink is deposited into the ink pan/tray. The doctor blade meters the ink flow onto the Anilox. The Anilox transfers a specified volume of ink onto the plate cylinder. The raised image on the plate cylinder transfers the ink on to the substrate, and forming the desired image. [10]

The main variable found in this process would be the Anilox roll. This roll is a hard cylinder, made of steel that contains very fine dimples called cells. These rolls can affect the quality of the print as they vary in cell shape and depth, which is usually associated as the cell volume. The other parameters that can affect the print with laboratory standard flexography machines are the print speed, the gap between the impression cylinders (known as the impression gap) and the ink used. In many of the laboratory scale flexography machines, it was found that the ink trays present were not enclosed, which affects prints using humidity sensitive inks.

F. Inks

There are many conductive inks, such as copper, silver and graphene ink, that can be considered for flexography. Copper ink has been popular for flexography printing, however research suggests that copper inks have a very long curing time and shows to have a higher resistance measurement than silver inks. [11] Carbon in the form of graphene ink can be considered. Although solid graphene sheets are known to have excellent conductive properties, graphene ink on the other hand has poor conductive properties. [12]

G. Surface Topography

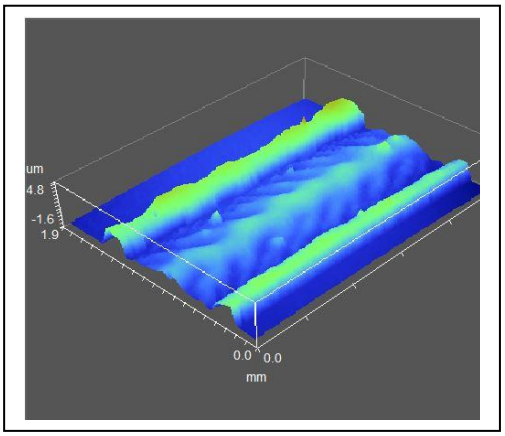

Figure 6. 3-Dimensional profile of an ink

Surface topography is the measurement of local deviations from a perfectly flat plate. [13] It can be used to characterise the shapes of inks and substrates, allowing to give a digital representation of the profile. Figure 6 shows a 3-D profile of a printed ink. The profile of the sample can be used to give measurements of roughness using the arithmetical mean deviations, the root mean square deviations, the maximum height and the total height of roughness profile. [14] The surface profile can also give measurements of the width and the height of the profile from analysis of its cross section.

Surface topography can be done by using a white light interferometer. It uses the interference effects occurred when light has been reflected by a reference mirror scanning through a set depth. [15] A common interferometry measurement technique is the vertical scanning interferometry, where the white light of low coherence is used. . Figure 6 shows a 3-D profile of a printed ink using white light interferometry.

III. MATERIALS

A. Substrates

There were two types of materials used as substrates for this research: Polyethylene terethalate (PET) and Polypropylene (PP). Table 1 shows the thickness and the

number of substrates produced. The substrates were cut to the dimension of the antenna template, 29.7 x 10.5 cm, with the use of a stencil cutter and a guillotine cutter. To ensure the substrate will not have any dust particles present, the substrates were then placed in a bath of isopropyl alcohol and then wiped with a lint free cloth. For this research, 21 substrates were cut for each material.

Table 1. Types of Substrate

	PET		PP
Thickness (μm)	175	50	59
No. of Substrates Cut	7	14	21

B. Ink

For this research, the Novacentrix PFI-772 ink was used. This is a water based conductive ink, containing silver nanoparticles, used specifically for flexography printing. This ink has been formulated to give high conductivity and minimal cured film thickness, which will reduce the amount of contact of silver in the antenna. Thus reducing the process cost of the tag. To ensure the print will have an even distribution of silver ink, the ink should be shaken thoroughly before use. [16]

C. Chip

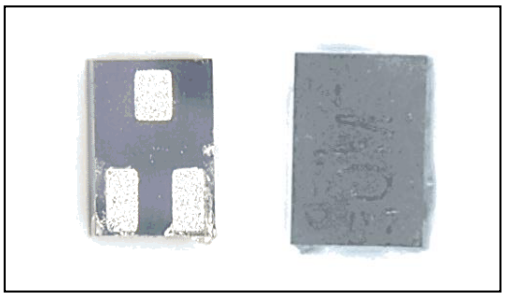

Figure 7. Image of G2XM chip

The transistor used in this research was the G2XM chip. Its applications consist of item level tagging, asset management, container identification, product authentication and supply chain management. It has high sensitivity allowing to give a longer read range. This chip has been manufactured specifically for a UHF RFID tag. The height, length and width of the chip are 1.45 mm x 1 mm x 0.5 mm respectively. [17]

D. Anilox Roll

There were three anilox rolls used in this research. Most of the anilox rolls that are available in the laboratory are 60-degree hexagonal shapes but differ in the size and depth. The rolls used in this research were 24 cm^3/m^2, 14 cm^3/m^2 and 8 cm^3/m^2 anilox rolls. It should be noted that the rolls should be cleaned straight after printing, using only water and soap, as the ink can oxidise in the cells resulting in its damage.

IV. Methodology

A. Plate Design

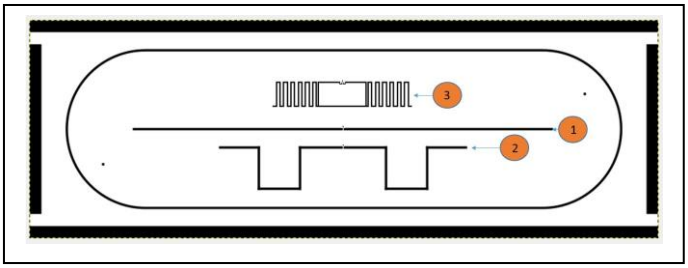

Fig 8. Antenna Template

In order for a substrate to have an antenna to be printed, a plate with the antenna design has to be printed. For ultra-high frequency RFID tags, the antennas are based on a half-wave dipole. [18] To design the antenna, the length of the dipole had to be determined first. Each pole length of the dipole can be determined approximately as a quarter of the measured wavelength. The wavelength of the desired frequency can be determined using equation (1), where: λ is the wavelength in meters, c is the speed of light and f is the frequency in Hertz. [19]

$$\lambda = c/f \quad (1)$$

European regulations have stated that for RFID tags produced must be in the range of 865.6 to 867.6 MHz, so following those regulations a frequency of 867 MHz was used. [20] The pole length of one side of the dipole was calculated as 8.65 cm. To make sure the size of the substrate would fit into the flexography machine used, the overall dimension of 29.7 x 10.5 cm was used. [21] The plate with the design template, will then be created with the use of digital and analogue printing processes, with a material made up of rubber or polymer. Figure 7 shows the three dipole antenna designs which will be used in the research. Each design consists of a different shape, but with the pole length of 8.65 cm. To make sure each print will be accurate to each other, impression dots were been placed diagonally to one another in the template as shown in figure 7.

B. Flexography Machine Set up

In this research, the RK Flexiproof 100 flexography machine was used. To attach the printing plate to the plate cylinder, double-sided adhesive tape was placed on the plate. When placing the tape on the plate any visible air pockets should be removed, as these pockets will create an uneven surface on the plate when printing. One edge of the plate should be placed just on the shaded line as shown in figure 9, ensure that the plate is positioned straight. The same plate will be used to print these antennas in this research to reduce any experimental errors and remain consistent.

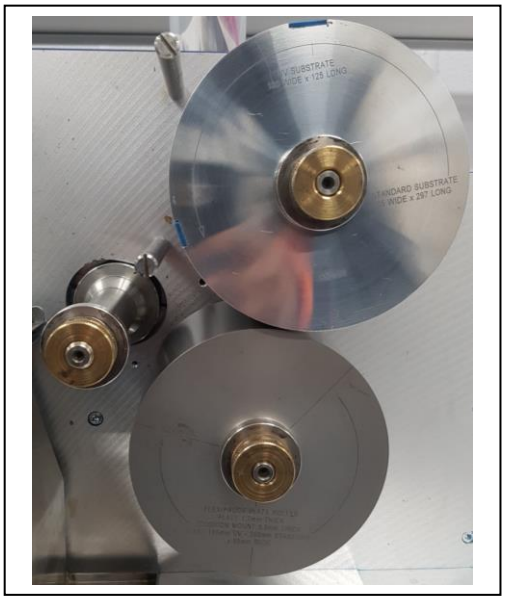

Figure 9, Impression roll

For the substrate to be positioned straight, the two edges of the width were pressed on the blue adhesive section of the impression roll. The mid-section were pressed on the second blue adhesive section as well, allowing the substrate to be as flat as possible. The speed of the print was set to 50 mm/min. The impression gap was set using the engagements of 65 and 72 for left and right respectively. The mounting tape used in this research was of 0.38 mm thickness. The first anilox roll used in this research was the $24cm^3/mm^2$. After placing the anilox roll on the station, the ink was be placed on to the ink tray with a pipette. After placing sufficient ink, the power was turned on allowing the rotating anilox roll to absorb the ink into its cells. Once the roll had been saturated with the ink, the two green start buttons were simultaneously. This ran the print, creating an imprint of the antenna on the substrate.

Each anilox roll was used to print 7 samples with each material. This is done to reduce experimental errors while measuring the resistance and the ink thickness, as the mean resistance and thickness can be taken for each print. To avoid oxidation of the ink, the ink tray should be regularly refilled while printing. Making practice prints on the flexography machine would be recommended, as it would allow the user to see if there could be any issues with the machine, such as the ink not being impressed onto the substrate well enough due to the impression gap being too wide.

C. Curing Process

Once the antennas were printed, the next step was to cure the substrates. The curing process allows the ink to dry, leaving the remaining conductive particles to harden on the substrate. For this research, the substrates were placed in a convection oven at 100 degrees Celsius for 15 minutes.

D. Resistance Reading Methodology

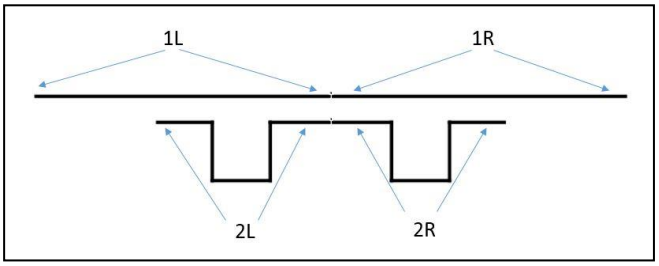

Figure 10. Illustration of Probe Positioning

The resistance of the ink was measured to analyse the resistance variance of the two designs shown in figure 10 and the different substrates used. The resistance was measured using a multimeter and two leads with probe ends. To take the readings, the multimeter was plugged into a power source and then the two leads were placed into the input and output section of the multimeter. Once the multimeter had been set, the resistance can be measured by placing the probe ends on each side of the probe length of position '1L' as shown in figure 10, for the first antenna sample. To attain reliable resistance readings, the mean of at least three should be taken. Once the readings for one pole length of the antenna is taken, measure the resistance for the three other pole lengths as shown in figure 10. This method should be repeated to measure the other 41 substrates. The magnitude of the compression of the probe when placing on the pole should be taken into consideration as it can scratch the ink, damaging the performance of the antenna.

E. WLS data collection

Figure 11. White Light Interferometer Instrument

The surface topology data was collected using white light interferometry and the WYKO Vision32 software. After providing a power source to the instrument and running the WYKO Vision32 software. The objective lens should be set to IX5 20% on the instrument. In the software, objective in the measurements options should be set to the serial number of the lens, which in this research was IX99520-5X. The field of view (FOV) was set to 0.5X, allowing the image measured to be the scale of the 1mm width of the printed ink width. The measurement technique used in this research was with vertical scanning interferometry (VSI). The backscan, length and modulation threshold used for the VSI options in this research were 25 um, 15 um and 3% respectively. After measurement

options have been set, the intensity should be set on the monitor to see the measuring sample on screen. Once the substrate with the antenna printed on has been placed the sample bed directly under the objective lens, the nob shown furthest away from the objective lens in figure 11, should be rotated moving the objective lens approximately a few centimetres away from the sample piece. It should be taken into consideration when moving the objective lens when setting the image with the nob, should be moved with care as the lens can get damaged as it can come into contact with the sampling bed. Once the image of the sample can be seen on the monitor, the focus nob, shown as the black nob closest to the objective lens, should be calibrated until fringes can be seen perpendicular to the antenna line. The data can be collected, after the intensity on the monitor does not show any shades of red, using the 'create new document' option.

The line width can be measured using the collected surface profile data using the Y-Profile in the 2D analysis option, as it gives a cross sectional view of the ink. To get accurate roughness values, a sub region of the ink section should be defined with at least a size of 400 micrometer x 400 micrometer, giving the mean deviation of roughness, the root mean square deviation of roughness, the maximum height of the roughness and the total height of the roughness profile.

F. Chip attachment

After collecting the resistance and ink surface profile, the chip can be attached between the dipole gaps, ideally using silver adhesive ink with the aid of a microscope. However, for this research the same ink used for printing the antennas was used as a substitute. The chip can be placed with the aid of a microscope. Once placing the substrate under the microscope, a dab of ink should be placed on the top edges between the dipole, using a needle. Care must be taken to not use excess ink as there could be a possibility of the ink overlapping with each other, which would not permit the chips to respond. Using a tweezer, the chip can be placed with the terminals facing the dabbed ink. It would be recommended to attempt practicing inking the chips to ensure how much ink will actually be needed as well as to get a better understanding of how to place the chips.

To measure the reading range of each antenna shape, it would be ideal to place one chip per tag, giving two tags with chips per antenna design, for each material. Once the chips have been placed on the antennas, the curing process has to be repeated again with the same parameters, to make sure the conductive ink hardens between the antenna and the transponder.

G. 2-Part Epoxy

To increase adhesion of the transponder on the tag, a 2-part epoxy was deposited onto the chip to seal it into position. The vapours from the 2-part epoxy were noted to be harmful and therefore the work was carried out in a fume cupboard. The epoxy hardens after 4 minutes after exposed to air, so a timer was used to keep track of time. Care was taken to ensure the ratio of the two liquids were close to 50:50, as there could be a risk of the silver ink degrading if exposed to higher quantities of either parts, resulting in a non-responsive tag. Once the liquids have been mixed thoroughly with wooden sticks, scoop the epoxy mixture with the stick and place around the chip in a spiral manner. It would be ideal to first practice on a few sample tags as initial attempts could be tricky due to the epoxy detaching the chip from the tag.

H. Reading Range Measurement

For the measurement of the reading range of the tag, a UHF desktop reader and a custom software called UHFReader09, which allows to read and write information on the tag, were used in this research. [22] Placing the straight edge perpendicular to the chip, the sensor was placed on top, touching the two-part epoxy, to check whether the tag is responsive. If the tag is responsive, the sensor will give a feedback with a sound. To evaluate the reading range, move the sensor with along the length of the ruler. Once the sensor stops giving the feedback, the reading range of the tag and the sensor have been identified. It would be suggested to measure the reading range 3 times and reduce error by taking the average of the measurements. It would also be recommended to use a plastic ruler as a metal ruler can affect the reading range of the antenna.

V. TEST RESULTS AND GRAPHICAL PRESENTATION

A. Resistance evaluation of printed ink

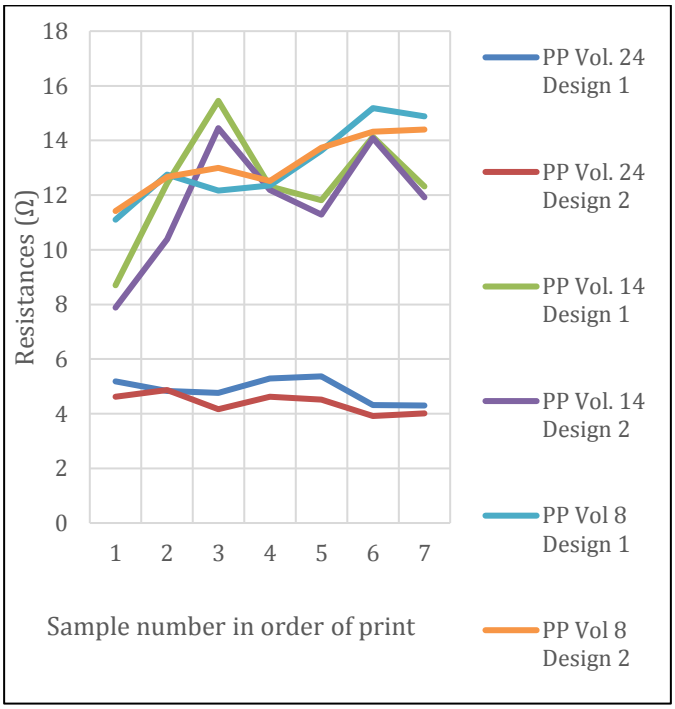

Figure 12.Average Resistance of Antenna Designs vs Print order for PP

Figure (12) shows the average resistance of design 1 and design 2 for each anilox roll for PP in order of print. It can be seen that the variation of the resistance between design 1 and 2 for all 3 anilox roll used is no more than 1 ohm. This implies that the resistance measured is not affected based on the design of the antenna.

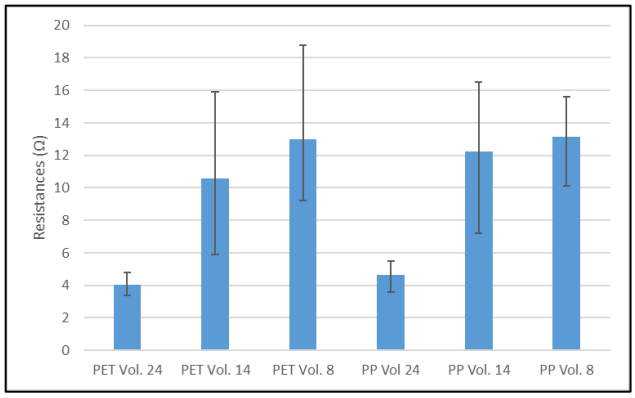

Figure 13. Average Resistance vs Anilox Volume

Figure (13) shows the average resistance of each substrate with different anilox rolls and the black vertical lines on the bar graph shows the standard deviations of the resistance. It can be seen that the resistance increases as the cell volume of the anilox roll decreases. The anilox roll with the cell volume of 24 shows the lowest resistance, with 4.04 and 4.6 ohms for PET and PP respectively, and also has the lowest amount of deviations as seen on graph for both PET and PP substrates. The anilox roll with the cell volume of 14 cm^3/m^2 shows a consistent amount of deviations between each substrate and has an average resistance of 10.57 and 12.2 ohms for PET and PP respectively. The anilox roll with the cell volume of $8cm^3/m^2$ has the highest average resistance, with 13.0 and 13.15 ohms for PET and PP respectively, however this shows an inconsistent range of deviations when comparing between the PET and PP substrates as PET varies with a range of 9.6 ohms, whereas PP only has a variance range of 5.5 ohms.

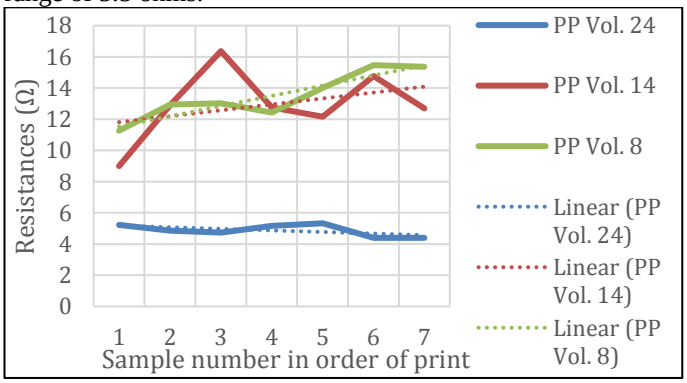

Figure 14. Average Resistance of Sample vs Print order for PP

Figure (14) shows the average resistance of PP substrates measured over the order of the antennas printed to see whether the ink had a consistent or a linear measure of resistance. It can be seen that the linear approximation of the average resistance of the cell volume $8m^3$ has a higher gradient than the anilox roll with the cell volume of $14cm^3$, however when comparing the average resistance by itself it has an inconsistent increase. The linear approximation of the average resistance of the cell volume of the 24 cm^3/m^2 has a decreasing gradient as the print order increases, but when comparing the average resistance of the cell volume of the anilox roll in order of the print, it has an inconsistent reading range. It can be seen that the maginitude of the linear approximation gradient is smaller in comparison to the cell volume of the $14cm^3$. Therefore it can be said that the magintude of the linear approximation gradient increases as the cell volume of the anilox roll used decreased.

B. Print Comparison of PET and PP

Table 2 Thickness of substrates used for printing antennas

Substrate	Anilox (cm3/m2)	Substrate Thickness (microns)
PP	24	59
PP	14	59
PP	8	59
PET	24	175
PET	14	50
PET	8	50

Table 2 indicates the thickness of the substrate used for each print.

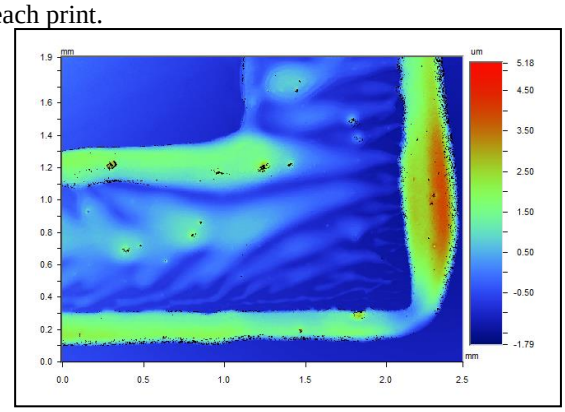

Figure 15 Ink Surface profile of Corner Section

Figure (15) shows surface profile indicating the ink formation on the corner section of the right hand side of antenna design 2, referenced to figure (8). It can be seen that there is a large ink deposition shown on the right side of figure (15). The black spots on the image indicate the areas where the white light was not able to collect the data from. This could potentially be due to interference.

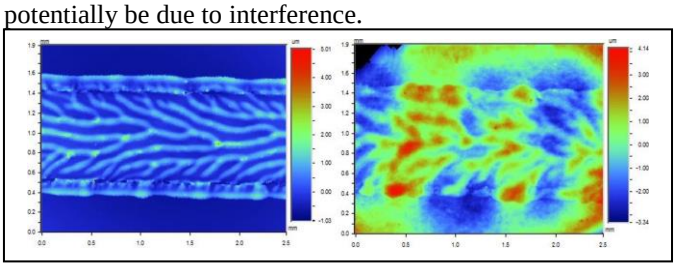

Figure 16. PET and PP Vol. 24 respectively.

Figure (16) shows an ink surface profile section of the left di-pole length in antenna design 1, for both PET and PP substrates printed with the anilox roll with $24cm^3/m^2$ cell volume. The colours in the image, in order of the light spectrum, indicates the height calculated using surface topology, with the bright red shade indicating the peaks and dark blue indicating the toughs in the profile. It can be seen in the ink of both surface profiles, in figure (16), that there is a smooth layer of ink present on the top and bottom ending sections of the ink. This pattern has occurred due to the excess ink collected by the template plate, from the anilox roll, being pressed on to the substrate, causing the excess ink to be pushed on to the sides of the impression of the template during the print. In between the top and bottom smooth finishing sections of both surface profiles, there is a well-defined pattern indicating viscous fingering in figure (16). [23]

There are 3 layers of red in the PP surface profile section, shown in figure (16), indicating the printed ink has an uneven layer of thicknesses. It can be seen that when measuring the height from the top to the mid-section of the surface profile, the colour changes from a light green shade to blue, indicating the height of the substrate is higher than the ink.

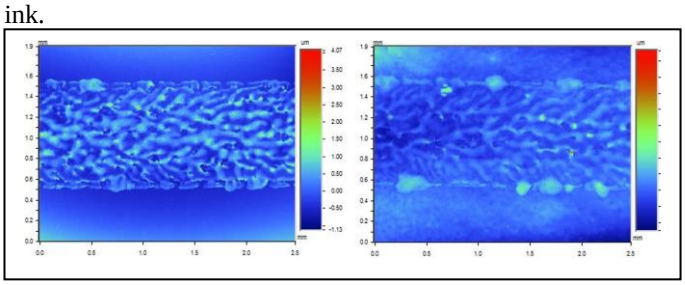

Figure 17. Surface Profile of PET and PP Vol. 14 shown respectively.

Figure (17) shows the ink surface profile section of the left di-pole length in antenna design 1, for both PET and PP substrates printed with the anilox roll with 14 cm^3/m^2 cell volume. It can be seen that the viscous fingering pattern in the ink has become less defined when comparing to figure (16). In the PP surface profile, in figure (17), on the right side of the ink, there is a section with where the height of the profile has a sudden increase. This has occurred due to a dust particle had been present when measuring the profile with the white light spectrometer.

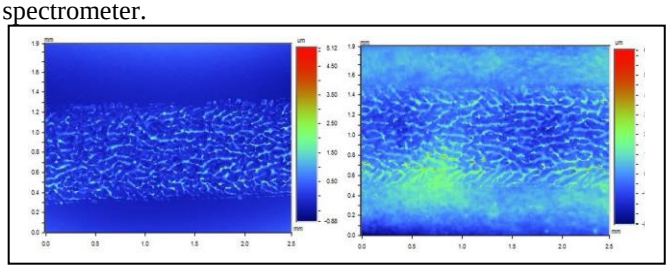

Figure 18. Surface Profile of PET and PP Vol 8 shown respectively.

Figure (18) shows the ink surface profile section of the left di-pole length in antenna design 1, for both PET and PP substrates printed with the anilox roll with 8 cm^3/m^2 cell volume. It can be seen that the viscous fingering pattern formed with the ink in figure (18) is very coarse with the least definition.

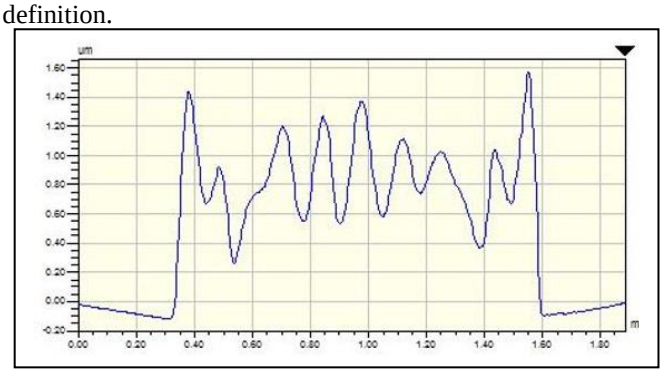

Figure 19 Cross-Sectional View of PET Vol 24.

Figure (19) shows the cross-sectional view of the ink at the left dipole length of antenna design 1, printed using PET with the anilox cell volume of 24 cm^3/m^2. It can be seen that the peaks in figure (19) have thick and tall features and when comparing the peaks of the ink from the centre to its sides, it can be seen that the peaks decrease in height until it reaches the side where it moves outwards at an angle and points upwards, resembling a 'rabbit ear pattern'.

Figure 20. Image and Cross-Sectional View of PET Vol 14

Figure (20) shows the cross-sectional view of the ink at the left dipole length of antenna design 1, printed using PET with the anilox cell volume of 14 cm^3/m^2. It can be seen that the cross section of the ink shown in figure (20) features more peaks and have taller peaks at the centre than its sides. The 'rabbit ear' pattern has shown to be less prominent as seen in figure (19).

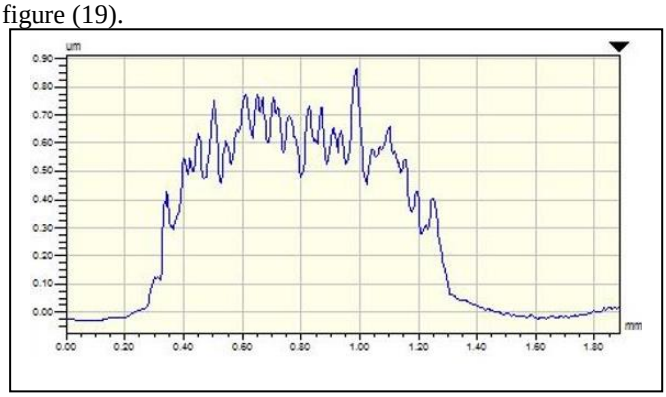

Figure (21). Cross-Sectional View of PET Vol 8

Figure (21) shows the cross-sectional view of the ink at the left dipole length in the antenna design 1 printed using PET with the anilox cell volume of 8 cm3/m2. It can be seen that the centre of the cross section of the printed ink shown in figure (21) have no resemblance of the 'rabbit ear' pattern and have the most amount of rigid peaks in comparison to figures 19 and 20.

C. Roughness Evaluation

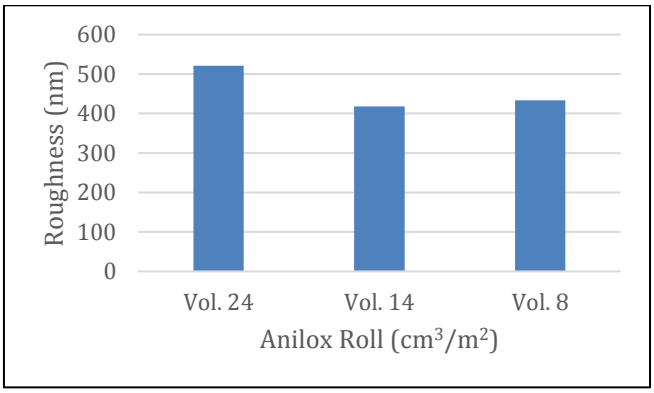

Figure 22. Average Roughness vs Anilox Volume

Figure (22) shows the Average surface roughness measured using the white light interferometer, for the varying anilox rolls used for PET substrates. The root mean square deviation

of the roughness profile was used to compare against the different anilox rolls used. It can be seen that there is an inconsistent decrease in roughness as the cell volume of the anilox roll with the decreases.

D. Line Width and Thickness Evaluation

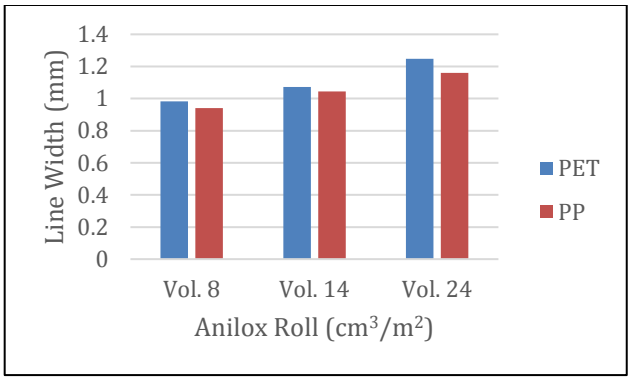

Figure (23). Line Width vs Anilox Volume for PET

Figure 23 shows the average line width of the varying anilox roll for PET and PP substrates. It can be seen that the line width increase as the anilox roll with a higher cell volume is used. It can also be seen that the line width of all three the PP substrates are lower than the line width of the PET substrates. This is due to the fact the ink had sunk into the warped substrates during the curing process. The line width of the PET and PP substrates with the ink printed with the 24 cm^3/m^2 cell volume anilox roll have a higher height than the other line width measurements due to the excess ink present on either side of the print as shown in figure (16).

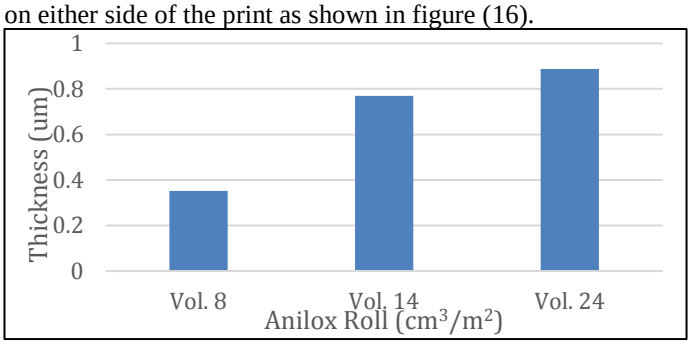

Figure 24. Film Thickness vs Anilox Roll for PET substrates.

Figure (24) shows the average film thickness measurements of the ink using the cross sectional area profiles. It can be seen that the thickness increases as the anilox roll with the cell volume increases. This is expected since the anilox roll with a higher cell volume will be able to collect more ink from the ink tray, allowing the template plate to place more ink on to a substrate than an anilox roll with a lower cell volume.

E. RFID reading range

Table (3). RFID Response range.

Substrate Type	Anilox Volume	Design Type	Range (cm)
PET	24	Design 2	2
PP	8	Design 1	6
PP	24	Design 2	Touch

Table (3) shows the reading range of the tags after the placement of the two-part epoxy, of the response range varying with the design type, substrate and cell volume of anilox roll used. It can be see that the design 1 antenna gives the longest reading range.

VI. Discussion of Results

A. Resistance and Anilox Volume

It was found that the resistance of the both PET and PP substrates had increased as the anilox roll with the cell volume had decreased. This is due to the fact that the amount of conductive particles present in the print were lower as less ink was used. Since there is only a resistance variance of 15.4 ohms between the varying anilox roll and substrates, the antenna performance should not be affected as much so for industrial use the 8 cm^3 can be used reducing the cost of the production of the antenna as less volume of silver is used. It was found that marks on the ink were seen when measuring the resistance using the probe resulting in removing some of the ink. This shows that the ink isn't highly durable on the substrate and in application, it would need to be sealed like the chips sealed with 2-part epoxy.

B. Print Comparison

It can be seen that in figure (16) the printed ink has an uneven layer of thicknesses and the height of the substrate is higher than the ink. This uneven layer has been caused due to the ink sinking into the substrate as the substrate warped due the high curing temperature. It was also seen in figure (16) the printed ink has an uneven layer of thicknesses. This has occurred due to the ink sinking into the warped substrate during the curing process. This can be overcome using a thicker substrate and decreasing the curing temperature but increasing curing time.

C. 'Rabbit Ear' and Viscous Fingering Pattern

Figure (16) In between the top and bottom excess ink sections of both surface profiles, there is a well-defined pattern indicating viscous fingering. It can also be seen that the cross section in figure (19) resembles a 'Rabbit Ear' pattern. It can be said that there is a correlation between the viscous fingering pattern and the 'rabbit ear' pattern, as the viscous fingering pattern becomes coarser as the 'rabbit ear' pattern becomes less prominent.

D. Corner Print of Antenna Design 2

Figure (15) shows the corner of the antenna to have a rounded corner. The antennas were designed to have sharp corners so it could be concluded that it is likely the ink has spread during the print and further work could be done to perfect the distance between the plate and impression cylinder.

E. Roughness, Thickness and Width

Due to the sinking of the ink in the warped substrates, the PP substrates were not able to give accurate white light interferometry readings. The results shown in figure (22) have shown to give no correlation with the results of the figures (16-21), as the coarse ink pattern and the rigid peaks both indicate that the roughness should decrease as the anilox roll with a higher cell volume is used. Due to the inconsistency of the results and the unavailability of the roughness measurements for the PP substrates the overall evaluation of roughness for all 3 inks for both substrates have been said to be inconclusive and requires further research.

It could be seen that line width and thickness increase as the anilox roll with a higher cell volume was used.

F. Chip attachment issues and effectiveness

It was found that the chips the convection oven had caused the conductive ink placed on the terminal of the chips attached had displaced, causing the tag to become non-responsive. Further research with the use of a static oven or using photonic curing could assist in keeping silver adhesive of chips on tags. It was found that prior to the 2-part epoxy placement on the chips, there were about 8 responsive RFID tags, but after the placement of epoxy most RFID tags apart for had become unresponsive or had a low reading range. This could be due to the fact the epoxy had not been mixed with a 50/50 ratio mixture. Another possibility of the reading range being low could be due to the heating of the chip during curing. It can be said that the chip attachment method is quite inefficient and unreliable as placement of one tag itself is very time consuming and sometimes more than one chip may be required as the ink could spread onto both terminals connecting them together making the transistor unusable.

VII. Conclusion

This research has successfully printed responsive RFID tags. It was found that the curing temperature had affected the PP substrates and the convection oven had caused the conductive ink placed on the terminal of the chips attached had displaced, causing the tag to become non-responsive. It was found that the resistance of the antenna decreases as the anilox roll with a higher cell volume count was used due to more conductive silver particles present. It was also seen that the line width of the antenna decreases as the anilox roll with a lower cell volume count was used. The reading range of the responsive tags increased as the size of the dipole had increased.

VIII. Future Research Recommendation

On completion of this research, it is recommended that in the future research should include:

- The potential use of a static oven or use ionic curing for drying the ink.
- Using thicker materials for printing antennas
- The potential use of atomic force microscopy for analysis of surface characterisation
- The analysis of the engagement gap to perfect the plate and the impression cylinder
- Possible aspect of mass production of the printable antenna, including the costs associated in with printing and chip writing.

Acknowledgments

I would firstly like to thank Dr. Davide Deganello for his expertise and supervision during my research. I would like to express my gratitude to Caitlin McCall for all her assistance in reaching my targets of my research. I would also like to give thanks to Sarah J. Potts for all her advice and for her expertise on the white light spectrometer. Lastly, I would also like to give my thanks to the WCPC lab members for all their additional support during my research.

References

[1] Merriam-Webster, Incorporated, “Merriam-Webster,” Merriam-Webster, Incorporated, 17 April 2018. [Online]. Available: https://www.merriam-webster.com/dictionary/radio%20frequency. [Accessed 29 April 2018].

[2] Atlas RFID Solutions, “The Basics of an RFID System,” [Online]. Available: http://rfid.atlasrfidstore.com/hs-fs/hub/300870/file-252314647-pdf/Content/basics-of-an-rfid-system-atlasrfidstore.pdf.

[3] E. Perret, “Design of Antennas for UHF RFID Tags,” Proceedings of the IEEE, 2012.

[4] E. Z, “RFID4u,” 27 September 2017. [Online]. Available: https://rfid4u.com/applications-for-active-and-passive-rfid/. [Accessed 22 April 2018].

[5] S. Smiley, “RFID Tag Antennas,” Atlas RFID, 14 February 2017. [Online]. Available: https://blog.atlasrfidstore.com/rfid-tag-antennas. [Accessed 30 January 2018].

[6] S. Armstrong, “RFID INSIDER, Tracking The RFID Industry,” Atlas RFID, 29 October 2012. [Online]. Available: https://blog.atlasrfidstore.com/which-rfid-frequency-is-right-for-your-application?utm_source=RFID_Basics&utm_medium=RFID_Basics_Link&utm_campaign=Content&utm_content=rfid_frequency. [Accessed 24 April 2018].

[7] F. Vander-Zante, “Skin Effect & Fields,” hamstudy, [Online]. Available: https://www.hamstudy.com/freeadvanced/a-001-2.html. [Accessed 26 April 2018].

[8] AMazing©, “Additive Manufactiuring,” AMazing©, [Online]. Available: http://additivemanufacturing.com/basics/. [Accessed 26 April 2018].

[9] R. C. Kattumenu, “Flexography Printing of Silver Based Conductive Inks on Packaging Substrates,” Western Michigan University, Michigan, 2008.

[10] S. Merilampi, L. Ukkonen, L. Sydanheimo, P. Ruuskanen and M. Kivikoski, “Analysis of Silver Ink Bow-Tie RFID tag Antenns Printed on paper Substrates,” Hindawi Publishing Corporation, Tampere, 2007.

[11] S. Farnsworth, “Curing Copper and Other Thin-Film Materials at Procuction Speeds,” Novacentrix, Austin, 2009.

[12] D. Savastano, “Printed Electronics NOW,” 11 July 2014. [Online]. Available: https://www.printedelectronicsnow.com/issues/2014-04/view_features/the-possibilities-of-graphene-in-printed-electronics/47774. [Accessed 29 April 2018].

[13] CorsonPedia Inc., “Corrosionpedia,” [Online]. Available: https://www.corrosionpedia.com/definition/1058/surface-topography.

[14] Olympus Corporation, “Roughness (2D) parameter,” OLYMPUS, [Online]. Available: http://www.olympus-ims.com/en/knowledge/metrology/roughness/2d_parameter/ . [Accessed 3 May 2018].

[15] Polytec, “White-Light Interferometry,” Polytec GmbH, [Online]. Available: https://www.polytec.com/uk/surface-metrology/technology/. [Accessed 3 May 2018].

[16] PChem® Conductive Inks for Printed Electronics, “PFI-722® Conduvtive Flexo Ink,” Noacentrix.

[17] NXP, “SL3ICS1002/1202, UCODE G2XM and G2XL,” NXP B.V., 2013.

[18] D. Deavours, “UHF RFID Antennas,” University of Kansas, Kansas, 2010.

[19] E. Kranakis, “Antennae Basics,” Carelton University, Ottawa, 2012.

[20] C. A. Repec, “Regulatory status for using RFID in the EPC Gen2 (860 to 960 MHz) band of the UHF spectrum,” GS1 Global Office, 2016.

[21] The TMI Group of Companies, “Flexiproof 100/UV, Modle 30-60,” Testing Machines, Inc., Delaware, 2015.

[22] Chafon, “Chafon,” Chafon, [Online]. Available: http://www.chafon.com/productdetails.aspx?pid=384. [Accessed 30 April 2018].

[23] E. Hrehorova, “Materials and Processes for Printed Electronics: Evaluation of Gravure Printing in Electronics Manufacture”.